SLAC–PUB–5430
February 1991
(A)

SIMULATIONS OF CRAB CROSSING IN STORAGE RINGS*

A. Piwinski †

Stanford Linear Accelerator Center
Stanford University, Stanford, California 94309

Abstract

The beam-beam interaction with a crossing angle and with a compensating crab angle is simulated and treated partially analytically. The crab angle is obtained by transversely deflecting cavities in one case and by a dispersion in the accelerating cavities in another case. Resonances which are excited by the action of the crab cavities are investigated. Tolerances for the cavity voltage and for the betatron phases between the cavities and the interaction point are discussed.

*Work supported in part by the department of energy
Contract DE-AC03-765F00515
† on leave from DESY, Hamburg, Germany

1 Introduction

In very high luminosity storage rings a large number of colliding bunches is desirable, and this requirement leads to a crossing angle configuration. The advantages of a crossing angle over head-on collision are a better shielding of the detectors from synchrotron radiation, a larger separation of the beams at the parasitic crossings and a greater independence of the optics in the two rings.

In the double ring DORIS I, however, it was found [1] that a crossing angle excites synchro-betatron resonances which are determined by

$$k\,\nu_\beta + m\,\nu_s = n \tag{1}$$

where k, m and n are integers and ν_β and ν_s are the betatron frequency (in the plane of the crossing angle) and the synchrotron frequency in units of the revolution frequency. These resonances are spread over the whole tune diagram and reduce the beam-beam limit and the currents.

With crab crossing the bunches are tilted so that they collide head-on. If the tilt angle is made by transversely deflecting cavities these cavities must have a betatron phase distance of $\pm\pi/2$ or an odd multiple of it from the interaction point to produce a bump for the tilt. This kind of crab crossing was first proposed as a way to increase the luminosity in linear colliders [2] and was then proposed for storage rings in order to avoid the synchro-betatron resonances [3]. In low energy storage rings the number of transversely deflecting cavities which are necessary for the crab angle is sufficiently small so that they will not occupy too much space or increase the impedance of the ring too much.

A second method to obtain a tilt angle was proposed in [4]. The orbit displacements at the interaction point are produced by a large dispersions in accelerating cavities on both sides of the interaction point so that no additional cavities are necessary. According to a somewhat modified theory the maxima of the two dispersions must have a phase distance from the interaction point of π or an odd multiple of π on one side and a phase distance of 2π or a multiple of 2π on the other side of the interaction point. The position of the cavities is then arbitrary, and one can use several cavities distributed over a larger region of betatron phase.

Since crab crossing has not yet been verified in an existing storage ring it was studied by means of computer simulations for transversely deflecting cavities and for round beams [4]. In particular, errors of the voltage of the crab cavities and of the betatron phase between cavities and interaction point were simulated in order to find the tolerances for these parameters. Numerical estimates were also made in [6]. In this note simulations for both methods of crab crossing are discussed, and the simulations are done for flat beams with an aspect ratio of 25 : 1.

2 Transversely deflecting cavities

2.1 Transformation of the coordinates

The changes of the coordinates in a crab cavity were calculated by

$$\delta x' = \frac{\phi\, s\, V}{\sqrt{\beta_{xc}\beta_x^*}} \tag{2}$$

$$\frac{\delta E}{E} = \frac{\phi\, x\, V}{\sqrt{\beta_{xc}\beta_x^*}} \tag{3}$$

where ϕ is half the crossing angle and $V \neq 1$ describes the deviation from the correct value. β_{xc} and β_x^* are the amplitude functions at the crab cavity and at the interaction point, respectively. The energy change follows from the transverse kick and from Maxwell's equations [5]. If the phase advance to the interaction point is $\pi/2$ and if V is 1, $\delta x'$ gives $\delta x^* = \phi\, s$ at the interaction point and that means that the bunch is tilted by an angle of ϕ. At the second cavity, after another phase advance of $\pi/2$, the tilt angle is zero and the remaining betatron angle of $-\delta x'$ is compensated by a kick of the same strength and of the same sign as in the first cavity. Also the energy change (Eq.(6)) obtained in the first cavity is compensated in the second cavity since x has now the opposite sign.

The change of the betatron angles and of the energy due to the beam-beam interaction is given by

$$\beta_x^*\delta x' = 2\pi\xi_x\, f_x(x + \phi\, s,\, y) \tag{4}$$

$$\beta_y^*\delta y' = 2\pi\xi_y\, f_y(x + \phi\, s,\, y) \tag{5}$$

$$\delta E = \phi\, E\, \delta x' \tag{6}$$

where ξ_x and ξ_y are the space charge parameters and the functions f_x and f_y are integrals given by

$$f_x = \frac{x}{1-v} \int_0^{1-v^2} \exp\Big(-a\lambda - \frac{b\lambda}{1-\lambda}\Big) \frac{d\lambda}{\sqrt{1-\lambda}} \tag{7}$$

$$f_y = \frac{y\, v}{1-v} \int_0^{1-v^2} \exp\Big(-a\lambda - \frac{b\lambda}{1-\lambda}\Big) \frac{d\lambda}{\sqrt{1-\lambda}^3} \tag{8}$$

and

$$v = \frac{\sigma_y}{\sigma_{xef}}, \quad a = \frac{1}{2}\frac{x^2}{\sigma_{xef}^2 - \sigma_y^2}, \quad b = \frac{1}{2}\frac{y^2}{\sigma_{xef}^2 - \sigma_y^2}, \quad \xi_{x,y} = \frac{r_e N_b \beta_{x,y}^*}{2\pi\gamma\sigma_{xef,y}(\sigma_{xef} + \sigma_y)}$$

with r_e = electron radius, N_b = number of particles per bunch, γ = relative particle energy and $\sigma_{xef} = \sqrt{\sigma_x^2 + \phi^2\sigma_s^2}$. The integrals are solved numerically, tabulated and interpolated linearly for each passage of a particle.

As in the rest of the ring, the coordinates between the crab cavities and the interaction point are transformed linearly. ν_s is 0.06 and ν_y, which has no influence on the horizontal synchro-betatron resonances, is 0.23. The ratio of bunch length to beam width is 54 and the ratio of the betatron oscillation energy to the synchrotron oscillation energy [5] is $(\sigma_x^{*2}\alpha_m\bar{R})/(\beta_x^*\nu_s\sigma_s^2) = 0.01$. Most of the simulations are done for 3000 revolutions and with 98 particles. Quantum fluctuation and damping are neglected since the rise times on a resonance are shorter than the damping time. Also the betatron phase variation seen by a particle due to its longitudinal motion is neglected, i.e. it is assumed that the ratio of bunch length to β_x^* is small. This is the worst case since for a larger bunch length the space charge forces are distributed over a larger betatron phase and the excitation of higher order resonances will be compensated partly [7].

2.2 Eigenvalues of the transformation matrix

In order to investigate the influence of the crab cavities on the beam stability without beam-beam interaction we consider the linear motion of the particles by means of the matrix formalism. The synchrotron and betatron oscillation can be described by the four coordinates x, $\tilde{x}$, s and $\tilde{s}$ where $\tilde{x}$ and $\tilde{s}$ are given by

$$\tilde{x} = \alpha x + \beta x', \qquad \tilde{s} = q\frac{\Delta E}{E} = \frac{\alpha_m \bar{R}}{\nu_s \sigma_s}\frac{\Delta E}{E}$$

with $\alpha = -\beta'/2$, α_m = momentum compaction factor and $\bar{R}$ = mean machine radius. The transformation matrices for the transversely deflecting cavities are then given by

$$M_{c1,2} = \begin{pmatrix} 1 & 0 & 0 & 0 \\ 0 & g_{t1,2}\beta_{1,2} & 0 & 0 \\ 0 & 0 & 1 & 0 \\ qg_{t1,2} & 0 & 0 & 1 \end{pmatrix} \tag{9}$$

where $g_{t1,2}$ is the longitudinal gradient of the transverse kick. The matrices for the sections between the cavities are given by

$$M_{s1,2} = \begin{pmatrix} v_{1,2}\cos\varphi_{1,2} & v_{1,2}\sin\varphi_{1,2} & 0 & 0 \\ -v_{1,2}\sin\varphi_{1,2} & v_{1,2}\cos\varphi_{1,2} & 0 & 0 \\ 0 & 0 & \cos\psi_{1,2} & -\sin\psi_{1,2} \\ 0 & 0 & \sin\psi_{1,2} & \cos\psi_{1,2} \end{pmatrix} \tag{10}$$

where $v_{1,2}$ is $\sqrt{\beta_{1,2}/\beta_{2,1}}$ and $\varphi_{1,2}$ and $\psi_{1,2}$ are the betatron and synchrotron phase advances, respectively. The synchrotron frequency is assumed to be small and the sign of ψ depends on the sequence of the coordinates s and $\tilde{s}$. Since we assume that there is no curvature between the cavities we set ψ_1=0 and $\psi_2 = \psi$. The product of the four matrices is then

$$M_t = M_{s2}M_{c2}M_{s1}M_{c1} \tag{11}$$

$$= \begin{pmatrix} \cos\varphi & \sin\varphi & b_1\sin\varphi + v_1 b_2 \sin\varphi_2 & 0 \\ -\sin\varphi & \cos\varphi & b_1\cos\varphi + v_1 b_2 \cos\varphi_2 & 0 \\ -q\sin\psi(g_{t1} + v_2 g_{t2}\cos\varphi_1) & -R_t\sin\psi & \cos\psi - b_1 R_t \sin\psi & -\sin\psi \\ q\cos\psi(g_{t1} + v_2 g_{t2}\cos\varphi_1) & R_t\cos\psi & \sin\psi + b_1 R_t\cos\psi & \cos\psi \end{pmatrix}$$

with $\varphi = \varphi_1 + \varphi_2$, $b_{1,2} = g_{t1,2}\sqrt{\beta_{1,2}}$ and $R_t = qv_2 g_{t2}\sin\varphi_1$. The four eigenvalues $exp\{\pm i\mu_{1,2}\}$ of M_t are given by

$$2\cos\mu_{1,2} = \cos\varphi + \cos\bar{\psi} \pm \sqrt{(\cos\varphi - \cos\bar{\psi})^2 - q\sin\psi\sin\varphi\left(b_1^2 + b_2^2 + 2b_1 b_2\cos\varphi_1\right)} \tag{12}$$

with

$$2\cos\bar{\psi} = 2\cos\psi + qb_1 b_2 \sin\psi\sin\varphi_1$$

$\mu_{1,2}$ can become complex and the eigenvalues of M_t can get an absolute value larger than one if $\sin\varphi$ is positive, i.e. in the case of a difference resonance [8]. $\sin\psi \approx \psi = 2\pi\nu_s$ is always positive. The width of the resonance is then with $\delta\varphi = 2\pi\delta\nu_x$

$$\delta\nu_x = \pm\sqrt{q(b_1^2 + b_2^2 + 2b_1 b_2\cos\varphi_1)}\big/2\pi \tag{13}$$

The resonance vanishes for $b_1 = b_2$ or $g_{t1}\sqrt{\beta_1} = g_{t2}\sqrt{\beta_2}$ and $\varphi_1 = \pi$, 3π, etc. The resonance width for errors of the gradients, the amplitude functions and the phase distances are given by

$$\delta\nu_x = \pm\sqrt{q}\left|g_{t1}\sqrt{\beta_1} - g_{t2}\sqrt{\beta_2}\right|/2\pi\,, \qquad \delta\nu_x = \pm g_t\sqrt{q\beta}\,\epsilon$$

with $g_t\sqrt{\beta} = g_{t1}\sqrt{\beta_1} = g_{t2}\sqrt{\beta_2}$ and $\epsilon = \varphi_1/2\pi - 1/2$.

2.3 Simulation results

Fig. 1 shows the increase of the horizontal betatron amplitudes as a function of the horizontal betatron frequency in the case of a horizontal crossing angle. The initial amplitudes are $6\,\sigma_x$. For perfect compensation the synchro-betatron resonances vanish completely. The remaining resonances are the quarter resonance and some other resonances which are excited by the nonlinear beam-beam forces.

Fig. 2 shows the increase of the vertical amplitudes as a function of the vertical betatron frequency in the case of a vertical crossing angle of the same magnitude ($2\times7.5\,$mrad). For perfect compensation the synchro-betatron resonances vanish again completely. Without compensation the increase is larger than for the horizontal crossing angel since the normalized crossing angle $\phi\,\sigma_y/\sigma_s$ is larger by a factor of 25. For the same normalized crossing angle of 0.4 and $\phi = 0.3\,$mrad the increase

is of the same order of magnitude as for the horizontal crossing angle as shown in Fig. 3.

In Fig. 4 the increase of the amplitudes is plotted for a crossing angle of 1.5 mrad and a normalized crossing angle of only 0.08. The increase is clearly smaller but there are still many synchro-betatron resonances which will reduce the lifetime of the beam if the aperture of the ring is not very large.

In all the following figures, the horizontal amplitudes are shown for a horizontal crossing angle of 2×7.5 mrad. Fig. 5 shows the root-mean-square deviation of 1200 particles having a Gaussian distribution at the beginning. In contrast to Fig. 1 the rms value or the beam width blows up on only a few synchro-betatron resonances. Only the first satellite of the integer and the two lowest satellites of the third order resonance ($\nu_x = (1 \pm \nu_s)/3$) enlarge the beam width noticeably. The reason for this behavior is the fact that there are always particles with increasing amplitudes and those with decreasing amplitudes depending on the phase between betatron and synchrotron oscillation. For small excitations the increase and the decrease compensate each other. This means that the synchro-betatron resonances do not influence the luminosity very much but reduce the lifetime of the beams.

Fig. 6 shows the dependence of the maximum amplitudes on the cavity voltage around the resonance $\nu_x = (1 + \nu_s)/3$ for an initial amplitude of $3\,\sigma_x$. The voltage is varied in steps of 10% of the completely compensating value in both cavities at the same time. In this case a small crossing angle remains at the interaction point which is equal to the crossing angle times the relative error. If only one cavity has an error the residual angle is smaller [5] but a tilt angle of the order of the residual angle will oscillate around the ring.

The dependence of the maximum amplitudes on the phase distance of the transverse cavities from the interaction point is shown in Fig. 7 for initial amplitudes of $6\,\sigma_x$. In the frequency region considered here several synchro-betatron resonances are very close to each other. The strongest resonances are $\nu_x = (1 - \nu_s)/5 = 0.1880$ and $\nu_x = (1 + 2\nu_s)/6 = 0.1866$ but there are also the resonances $\nu_x = (1 + 5\nu_s)/7 = 0.1857$, $\nu_x = 1/8 + \nu_s = 0.1850$ and some other higher order resonances. Here again equal errors on both sides of the interaction point are assumed which are varied in steps of 3.6°. If the two cavities have position errors the beams will not only collide with a small angle but a small tilt angle will also oscillate around the ring. The error of the tilt at the interaction point can be compensated by varying the voltage of the two cavities which increases, however, the oscillation of the tilt around the ring.

In Fig. 8 the maximum amplitudes as found in Fig. 6 are plotted as a function of the cavity voltage for two different initial amplitudes. It shows that the dependence is stronger for larger amplitudes. Fig. 9 shows the dependence on position errors for the same resonance.

Figs. 10 and 11 show the dependence of the maximum amplitudes on the cavity voltage and on position errors for the resonances considered in Fig. 7. The dependence is stronger in this case where several resonances are very close to each other.

It will be difficult to compensate these resonances, and these few frequencies must be avoided.

Table 1 shows the tolerable errors of the cavity voltage and the phase distance for two synchro-betatron resonances.

$\Delta\hat{x}$	10 %		50 %		100 %	
ΔU	2.5 %	0.5 %	10 %	2 %	30 %	8 %
$\Delta\psi$	1.5^o	0.5^o	8^o	1^o	25^o	2.5^o

Table 1: Increase of amplitudes for different errors of the cavity voltage U and the phase distance ψ on the two resonances $3\nu_x - \nu_s = 1$ and $5\nu_x + \nu_s = 1$.

Figs. 12 and 13 show the maximum betatron amplitudes with the beam-beam interaction turned off on two satellites resonances of the integer. The voltage in only one cavity is changed in steps of 1 % of its nominal value from 90 to 100%. Whereas on the sum resonance $\nu_x + \nu_s$ = integer (Fig.12) the amplitudes approach an upper limit they increase continuously with the error on the difference resonance $\nu_x - \nu_s$ = integer (Fig.13). In the second case they increase also with the number of revolutions since on the difference resonance the particle motion is unstable (Eq.(12)).

2.4 Dispersion in transversely deflecting cavities

If there is a dispersion at the crab cavity one has to distinguish two cases. If the dispersion is produced outside of the crab bump it will not excite synchro-betatron resonances since this dispersion has the same phase advance as the betatron oscillation and the two kicks will compensate each other. If the dispersion is produced between the two cavities the two kicks will not compensate each other and a satellite resonance of the integer can be excited which gives an exponential increase for the difference resonance ($\nu_x - \nu_s$=integer) and an exchange of oscillation energy on the sum resonance ($\nu_x + \nu_s$=integer) [8].

If a bend between the two cavities produces a dispersion of a few centimeters, the effect due to this cause must be compared with that from the dispersion in the main accelerating cavities where a spurious dispersion of a few centimeters usually cannot be avoided. Since the excitation of synchro-betatron resonances is approximately proportional to the dispersion as well as to the gradient of the voltage [8], the excitation in the accelerating cavities will be larger than the excitation in the crab cavities by an order of magnitude. In any case, the first satellite of the integer must be avoided.

3 Dispersion in accelerating cavities

3.1 Transformation of the coordinates

The tilt angle can also be produced by an energy change at a position with a dispersion [5]. At first the tilt angle was calculated due to a change of the betatron coordinate x given by $\delta x = -D\,\delta E/E$. However, this is only half the effect. There is also a change of the betatron angle x' due to the derivative of the dispersion given by $\delta x' = -D'\,\delta E/E$, and the total change can be written in the form

$$\delta x = -D\frac{\delta E}{E} \qquad (14)\,, \qquad\qquad \delta\tilde{x} = -\tilde{D}\frac{\delta E}{E} \qquad (15)$$

with the abbreviations

$$\tilde{x} = \alpha x + \beta x'\,, \qquad\qquad \tilde{D} = \alpha D + \beta D'$$

Since in a straight section the dispersion is a free betatron oscillation we can write

$$D = a\sqrt{\beta}\cos(\varphi) \qquad (16)\,, \qquad\qquad \tilde{D} = -a\sqrt{\beta}\sin(\varphi) \qquad (17)$$

where a is a constant and φ is the betatron phase advance and is measured from a position where $\tilde{D}$ is zero and D is positive. A change of the betatron coordinates produced at position s_1 yields at the interaction point

$$\delta x_1^* = -a_1\sqrt{\beta^*}\,\cos(\varphi_1 + \Delta\varphi_1)\,\frac{\delta E_1}{E} \qquad (18)$$

$$\delta\tilde{x}_1^* = a_1\sqrt{\beta^*}\,\sin(\varphi_1 + \Delta\varphi_1)\,\frac{\delta E_1}{E} \qquad (19)$$

where $\Delta\varphi_1$ is the phase advance between the energy change and the interaction point. Since the sum $\varphi_1 + \Delta\varphi_1$ does not depend on the phase where the energy was changed the position of the cavity is completely arbitrary within the straight section.

The tilt angle is $\delta x^*/s$ which gives, with $\varphi_1 + \Delta\varphi_1 = \pi$, $a_1\sqrt{\beta^*}g_{\ell 1}$ where $g_{\ell 1}$ is the longitudinal gradient of the energy change in the cavity. If the tilt angle is half the crossing angle one gets

$$\phi = g_{\ell 1}\sqrt{\frac{\beta^*}{\beta_1}\left(D_1^2 + \tilde{D}_2^2\right)} \qquad (20)$$

If we compare the gradients in the accelerating cavities and in the transversely deflecting cavities which are necessary for the crab crossing we get $g_{\ell 1}/g_{t1} = \beta_1/D_1$ where equal amplitude functions for both cases are assumed and the dispersion is

evaluated at its maximum. The necessary gradient in the accelerating cavities is then larger by about an order of magnitude than in the transversely deflecting cavities.

We assume that the dispersion vanishes at the interaction point. A dispersion with the same phase at the interaction point (with respect to the phase in the cavity) will reduce the tilt angle and a dispersion with an opposite phase will increase it.

At the second cavity the transformation of the change produced at the first cavity gives

$$\delta x_1 \;=\; -a_1\sqrt{\beta_2}\,\cos(\varphi_1+\Delta\varphi_1+\Delta\varphi_2)\,\frac{\delta E_1}{E} \tag{21}$$

$$\delta \tilde{x}_1 \;=\; a_1\sqrt{\beta_2}\,\sin(\varphi_1+\Delta\varphi_1+\Delta\varphi_2)\,\frac{\delta E_1}{E} \tag{22}$$

where $\Delta\varphi_2$ is the phase advance from the interaction point to the second cavity. The change in the second cavity is given by

$$\delta x_2 \;=\; -a_2\sqrt{\beta_2}\,\cos(\varphi_2)\,\frac{\delta E_2}{E} \tag{23}$$

$$\delta \tilde{x}_2 \;=\; a_2\sqrt{\beta_2}\,\sin(\varphi_2)\,\frac{\delta E_2}{E} \tag{24}$$

where φ_2 is also measured from a position where $\tilde{D}$ vanishes and D is positive. The changes in the two cavities compensate each other if the two conditions are satisfied:

$$a_1\frac{\delta E_1}{E} \;=\; -(-1)^n a_2\frac{\delta E_2}{E} \tag{25}$$

$$\varphi_2 \;=\; \varphi_1+\Delta\varphi_1+\Delta\varphi_2+n\,\pi \tag{26}$$

Here n is an integer. The sum of the phase advance between the first maximum and the interaction point ($\varphi_1+\Delta\varphi_1$) and of the phase advance between the interaction point and a maximum on the other side ($\Delta\varphi_2-\varphi_2$) must be equal to a multiple of π, i.e. the phase difference between the two dispersions must be equal to $n\pi$.

The energy changes are given, in linear approximation, by the longitudinal position of the particle times the gradient of the voltage:

$$\frac{\delta E_1}{E} \;=\; g_{\ell 1}s_1 \tag{27}$$

$$\frac{\delta E_2}{E} \;=\; g_{\ell 2}\Big(s_1-A_1x-B_1\tilde{x}-\alpha_1 C(\frac{\Delta E}{E}+g_{\ell 1}s_1)\Big) \tag{28}$$

where α_1 is the momentum compaction factor for this section, C is the circumference and A_1 and B_1 determine the path lengthening due to the betatron oscillation (see Appendix A). Since there is no path lengthening in a straight section we may take the phase difference $\Delta\varphi$ between arbitrary points in the straight section, for instance between the two maxima, and get:

$$A_1 \;=\; 0\,, \qquad\qquad B_1 \;=\; \frac{D_2}{\sqrt{\beta_1\beta_2}}+\frac{D_1}{\beta_1}$$

Whereas α_1 can be minimized or maybe made equal zero, B_1 cannot become zero and this means that there remains a coupling.

The following transformations are used for the simulations. At the two cavities the coordinates are changed by

$$\delta x \;=\; -D_{1,2}\, g_{\ell 1,2}\, s \tag{29}$$

$$\delta \tilde{x} \;=\; -\tilde{D}_{1,2}\, g_{\ell 1,2}\, s \tag{30}$$

$$\delta E/E \;=\; g_{\ell 1,2}\, s \tag{31}$$

From the cavity to the interaction point the horizontal betatron coordinates are transformed linearly with a phase advance of $\Delta\varphi_1$ which is varied around π. The longitudinal coordinate is changed by

$$\delta s \;=\; -B_1\, \tilde{x} - \alpha_1\, C\, \Delta E/E \tag{32}$$

with

$$B_1 \;=\; D_1/\beta_1$$

A_1 is zero since we put the cavities at positions where $\tilde{D}$ vanishes. This simplifies the simulations. At the interaction point Eqs.(4), (5) and (6) are applied. From the interaction point to the second cavity the transformation is given by

$$\delta s \;=\; -A_2\, x - B_2\, \tilde{x} - \alpha_2\, C\, \Delta E/E \tag{33}$$

with

$$A_2 \;=\; D_2 \sin(\Delta\varphi_2)/\sqrt{\beta_2\beta^*} \qquad B_2 \;=\; -D_2 \cos(\Delta\varphi_2)/\sqrt{\beta_2\beta^*}$$

whereas the horizontal betatron coordinates are again transformed linearly with a phase advance of $\Delta\varphi_2$ which is varied around 2π. The transformation for the rest of the ring is a linear transformation with a phase advance $\Delta\varphi_3 = 2\pi\nu_x - \Delta\varphi_1 - \Delta\varphi_2$ for the horizontal betatron coordinates. The transformation for the vertical plane is always done at the interaction point for one revolution with a phase advance of $2\pi\nu_y$. The longitudinal coordinate is changed by

$$\delta s \;=\; -A_3 x - B_3 \tilde{x} - \alpha_3 C \Delta E/E \tag{34}$$

with

$$A_3 \;=\; D_2 \sin(\Delta\varphi_3)/\sqrt{\beta_2\beta_1} \qquad B_3 \;=\; -D_2 \cos(\Delta\varphi_3)/\sqrt{\beta_2\beta_1} + D_1/\beta_1$$

and $\alpha_3 = \alpha_m - \alpha_1 - \alpha_2$. If the total acceleration voltage is not necessary for the tilt angle the difference can be added at a position without dispersion which does not change the simulation results.

3.2 Eigenvalues of the transformation matrix

We consider now the influence of the dispersion on the stability of the particle motion without beam-beam interaction. The synchrotron and betatron oscillation are described again by the four coordinates x, $\tilde{x}$, s and $\tilde{s}$, and the transformation matrices for the two cavities are given by

$$M_{\ell c1,2} = \begin{pmatrix} 1 & 0 & -g_\ell D_{1,2} & 0 \\ 0 & 1 & -g_\ell \tilde{D}_{1,2} & 0 \\ 0 & 0 & 1 & 0 \\ 0 & 0 & qg_\ell & 1 \end{pmatrix} \tag{35}$$

where g_ℓ is the longitudinal gradient of the energy change which is assumed to be equal in both cavities. This is not a restriction since different gradients are equivalent to different amplitudes of the dispersions which are arbitrary. The matrices for the sections between the cavities are given by

$$M_{\ell s1,2} = \begin{pmatrix} v_{1,2}\cos\varphi_{1,2} & v_{1,2}\sin\varphi_{1,2} & 0 & 0 \\ -v_{1,2}\sin\varphi_{1,2} & v_{1,2}\cos\varphi_{1,2} & 0 & 0 \\ -A_{1,2} & -B_{1,2} & 1 & -\alpha_{1,2}C/q \\ 0 & 0 & 0 & 1 \end{pmatrix} \tag{36}$$

where $v_{1,2}$ is $\sqrt{\beta_{1,2}/\beta_{2,1}}$ and $\varphi_{1,2}$ is the betatron phase advance. We assume a betatron phase advance of 3π between the two cavities whereas the phase between the two dispersions is arbitrary. $A_{1,2}$ and $B_{1,2}$ are given by (see Appendix A)

$$A_1 = -\frac{\tilde{D}_1}{\beta_1} - \frac{\tilde{D}_2}{v_1\beta_2}, \qquad A_2 = -\frac{D_1\sin\varphi + \tilde{D}_1\cos\varphi}{v_2\beta_1} - \frac{\tilde{D}_2}{\beta_2}$$

$$B_1 = \frac{D_1}{\beta_1} + \frac{D_2}{v_1\beta_2}, \qquad B_2 = \frac{D_1\cos\varphi - \tilde{D}_1\sin\varphi}{v_2\beta_1} + \frac{D_2}{\beta_2}$$

The product of the four matrices is

$$M_\ell = M_{\ell s2}M_{\ell c2}M_{\ell s1}M_{\ell c1}$$

$$= \begin{pmatrix} \cos\varphi - v_1A_1I_2 & \sin\varphi - v_1B_1I_2 & -I_1 + v_1h_1I_2 & -v_1I_2\alpha_1C/q \\ -\sin\varphi - v_1A_1J_2 & \cos\varphi - v_1B_1J_2 & -J_1 + v_1h_1J_2 & -v_1J_2\alpha_1C/q \\ v_2A_2 - h_2A_1 & v_2B_2 - h_2B_1 & -g_l\alpha_2C + R_\ell & -(\alpha_1h_2 + \alpha_2)C/q \\ -qg_\ell A_1 & -qg_\ell B_1 & qg_\ell(1+h_1) & 1 - g_\ell\alpha_1C \end{pmatrix} \tag{37}$$

with $\varphi = \varphi_1 + \varphi_2 = 3\pi + \varphi_2$ and

$$I_{1,2} = g_\ell(D_{1,2}\cos\varphi + \tilde{D}_{1,2}\sin\varphi)\,, \qquad J_{1,2} = g_\ell(\tilde{D}_{1,2}\cos\varphi - D_{1,2}\sin\varphi)$$

$$R_\ell = h_1 h_2 - g_\ell(D_1 A_2 + \tilde{D}_1 B_2)\,, \qquad h_{1,2} = 1 - g_\ell\alpha_{1,2}C + g_\ell(D_{1,2}A_{1,2} + \tilde{D}_{1,2}B_{1,2})$$

The four eigenvalues $exp\{\pm i\mu_{1,2}\}$ of M_ℓ are given by

$$2\cos\mu_{1,2} = \cos\bar{\varphi} + \cos\bar{\psi} \pm \sqrt{(\cos\bar{\varphi} - \cos\bar{\psi})^2 + S} \tag{38}$$

with

$$2\cos\bar{\varphi} = m_{\ell 11} + m_{\ell 22}\,, \qquad 2\cos\bar{\psi} = m_{\ell 33} + m_{\ell 44}$$

where $m_{\ell ij}$ are the elements of the matrix M_ℓ. The most important term is S which determines the stability of the motion. It is given by

$$S = 2 - a_{\ell 11}a_{\ell 22} + a_{\ell 12}a_{\ell 21} - a_{\ell 33}a_{\ell 44} + a_{\ell 34}a_{\ell 43} + a_{\ell 13}a_{\ell 31} + a_{\ell 14}a_{\ell 41} + a_{\ell 23}a_{\ell 32} + a_{\ell 24}a_{\ell 42} \tag{39}$$

In order to simplify the calculation we define the following quantities

$$G_o = g_\ell\frac{D_1 D_2 + \bar{D}_1\bar{D}_2}{v_2\beta_1}\sin\varphi\,, \quad G_{1,2} = g_\ell\frac{D_{1,2}^2 + \bar{D}_{1,2}^2}{\beta_{1,2}}\sin\varphi\,, \quad T = g_\ell\frac{D_1\bar{D}_2 - \bar{D}_1 D_2}{v_2\beta_1}$$

Then we consider three cases. First we set $G_1 = G_2 = G_o = G$, i.e. we assume equal dispersions in phase and amplitude and get

$$S = -2g_\ell\alpha_1 CG(1 - \cos\varphi - g_\ell\alpha_2 C - G) \tag{40}$$

On the resonance is $\cos\bar{\varphi} = \cos\bar{\psi}$ which gives

$$2\cos\varphi = 2 - 2g_\ell\alpha_m C - 2G + g_\ell\alpha_1 C(g_\ell\alpha_2 C + G) \tag{41}$$

with $\alpha_m = \alpha_1 + \alpha_2$ and S becomes

$$S = -g_\ell^2\alpha_1^2 C^2 G(2 - g_\ell\alpha_2 C - G) \tag{42}$$

S is negative for $\sin\varphi > 0$ since $g_\ell\alpha_2 C + G$ is smaller than 2.

Secondly we consider $\alpha_1 = 0$ and $T = 0$, i.e. different amplitudes of the dispersions, and get

$$S = 2(1 - \cos\varphi)(G_o - G_1) + (g_\ell\alpha_2 C + G_o)(G_1 - G_2) \tag{43}$$

On the resonance one obtains

$$2\cos\varphi = 2 - 2g_\ell\alpha_m C + G_1 - 2G_0 - G_2 \tag{44}$$

and

$$S = -(\sqrt{G_1} - \sqrt{G_2})^2(g_\ell \alpha_m C - G_1) \tag{45}$$

which is also negative for $\sin\varphi > 0$.

Finally we consider the case $\alpha_1 = 0$ and $G_1 = G_2 = G \neq G_o$, i.e. phase errors of the dispersions, and obtain on the resonance

$$2\cos\varphi = 2 - (2 - T)(g_\ell \alpha_2 C + G_o - T\cos\varphi) \tag{46}$$

and

$$S = -g_\ell \alpha_2 C\,(G - G_o) \tag{47}$$

For S we have neglected all nonlinear terms in G, G_o and T. S is negative for $\sin\varphi > 0$ since G is larger than G_o ($G^2 = G_o^2 + T^2 \sin^2\varphi$).

On the resonance S becomes negative in all three cases and this means that on a difference resonance ($\sin\varphi > 0$) the phase μ of the eigenvalues becomes complex and their absolute values become larger than one. Therefore, an error in amplitude or phase of the dispersion and also a momentum compaction between the cavities causes an exponential increase of particle amplitudes on the difference resonance.

3.3 Simulation results

The simulations show that the compensation of synchro-betatron resonances with a dispersion in accelerating cavities gives similar results as the compensation with transversely deflecting cavities. The compensation as shown in Fig. 1 is also obtained with a dispersion in accelerating cavities and it is not necessary to show all the plots again. The dependence on errors is similar in both cases. As an example Fig. 14 shows the dependence of the maximum amplitudes on phase errors of the dispersions on the same resonances which are considered in Fig. 7. The phases on both sides of the interaction point are changed in steps of 3.6^o as in Fig. 7. The ratio $D/\sqrt{\beta_{xc}\beta_x^*}$ is 0.5 and the bending is assumed to be zero.

Figs. 15 and 16 show the maximum amplitudes as a function of the cavity voltage and phase errors. The dependence is roughly the same as in the case of transversely deflecting cavities shown in Figs. 10 and 11.

4 Conclusion

The simulations as well as the experiments with DORIS I have shown that the synchro-betatron resonances excited by the beam-beam interaction with a crossing angle reduce mainly the lifetime and do not affect seriously the beam size or the luminosity. Three parameters are important. The reduction of the lifetime is determined by the normalized crossing angle $\phi\,\sigma_\ell/\sigma_x$, the beam-beam space charge

parameter ξ_x and the physical or dynamical acceptance of the ring. If the normalized crossing angle is not larger than 0.5, the space charge parameter not larger than 0.03 and the acceptance not smaller than $15\,\sigma_x$, it should be possible to suppress almost all synchro-betatron resonances with reasonable tolerances for the transversely deflecting cavities or the dispersive cavities. If the acceptance is in the order of 20 to $30\,\sigma_x$ an operation with crossing angle but without crab cavities seems feasible.

There are only a few resonances for which a compensation is difficult, these resonances should be avoided. One of these resonances is the first satellite of the integer $\nu_x = \mathrm{n}+\nu_s$ on which the amplitudes increase exponentially for the smallest error of the crab parameters, with and without beam-beam interaction. Since an unavoidable spurious dispersion in all cavities causes the same effect this does not pose additional restriction.

References

1.) A. Piwinski,IEEE Trans. on Nucl.Sci. NS-24, 1408(1977)
2.) R. Palmer, SLAC-PUB-4707(1988)
3.) K. Oide, K. Yokoya, SLAC-PUB-4832(1989)
4.) G. Jackson, AIP Conference Proceedings 214(1990)
5.) A. Piwinski, DESY HERA 90-04(1990)
6.) S.A. Kheifets, J.M. Paterson, G.-A. Voss, SLAC-PUB-5011(1989)
7.) D. Sagan, R. Siemann, S. Krishnagopal, CLNS 90/1001(1990)
8.) A. Piwinski, A. Wrulich, DESY 76/07(1976)

Appendix A

The path lengthening between two arbitrary positions s_1 and s_2 is given by [8]

$$dL = \int_{s_1}^{s_2} \frac{x}{\rho} d\sigma = \int_{s_1}^{s_2} \frac{\sqrt{\epsilon\beta}}{\rho} \cos(\varphi) d\sigma \qquad (A1)$$

where ρ is the radius of curvature. Eq.(A1) can be written as

$$dL = \cos(\varphi_1 + \pi\nu) \int_{s_1}^{s_2} \frac{\sqrt{\epsilon\beta}}{\rho} \cos(\Phi_1) d\sigma \; - \; \sin(\varphi_1 + \pi\nu) \int_{s_1}^{s_2} \frac{\sqrt{\epsilon\beta}}{\rho} \sin(\Phi_1) d\sigma \qquad (A2)$$

with

$$\Phi_{1,2} = \Phi_{1,2}(\sigma) = \varphi(\sigma) - \varphi(s_{1,2}) - \pi\nu$$

If $f(\sigma)$ is a periodic function with a period length of C one obtains:

$$I = \int_{s_1}^{s_2} f(\sigma) e^{i\Phi_1(\sigma)} d\sigma = \int_{s_1}^{s_1+C} f e^{i\Phi_1} d\sigma - \int_{s_2}^{s_2+C} f e^{i\Phi_1} d\sigma + \int_{s_1+C}^{s_2+C} f e^{i\Phi_1} d\sigma$$

$$= \int_{s_1}^{s_1+C} f e^{i\Phi_1} d\sigma \; - \; e^{i\varphi_2 - i\varphi_1} \int_{s_2}^{s_2+C} f e^{i\Phi_2} d\sigma + e^{i2\pi\nu} I \qquad (A3)$$

and

$$I = \frac{1}{2\sin(\pi\nu)} e^{-i\pi\nu} \left(\int_{s_1}^{s_1+C} f e^{i\Phi_1} d\sigma - e^{i\varphi_2 - i\varphi_1} \int_{s_2}^{s_2+C} f e^{i\Phi_2} d\sigma \right) \qquad (A4)$$

With $f(\sigma) = \sqrt{\beta(\sigma)}/\rho(\sigma)$ and

$$D(s) + i\tilde{D}(s) = \frac{\sqrt{\beta(s)}}{2\sin(\pi\nu)} \int_{s}^{s+C} f(\sigma) \exp\left\{ i(\varphi(\sigma) - \varphi(s) - \pi\nu) \right\} d\sigma \qquad (A5)$$

one gets

$$\begin{aligned} I &= i e^{-i\pi\nu} \left(\frac{D_1 + i\tilde{D}_1}{\sqrt{\beta_1}} - e^{i\Delta\varphi} \frac{D_2 + i\tilde{D}_2}{\sqrt{\beta_2}} \right) \\ &= \frac{D_1 \sin(\pi\nu) - \tilde{D}_1 \cos(\pi\nu)}{\sqrt{\beta_2}} + \frac{D_2 \sin(\Delta\varphi - \pi\nu) + \tilde{D}_2 \cos(\Delta\varphi - \pi\nu)}{\sqrt{\beta_2}} \\ &+ i \frac{D_1 \cos(\pi\nu) + \tilde{D}_1 \sin(\pi\nu)}{\sqrt{\beta_1}} - i \frac{D_2 \cos(\Delta\varphi - \pi\nu) - \tilde{D}_2 \sin(\Delta\varphi - \pi\nu)}{\sqrt{\beta_2}} \end{aligned} \qquad (A6)$$

with $\Delta\varphi = \varphi_2 - \varphi_1$. Eqs.(A2) and (A6) yield

$$\begin{aligned} dL &= \sqrt{\epsilon} \cos(\varphi_1 + \pi\nu) \, Re\{ I \} - \sqrt{\epsilon} \sin(\varphi_1 + \pi\nu) \, Im\{ I \} \\ &= \sqrt{\epsilon} \left(\frac{-D_1 \sin(\varphi_1) - \tilde{D}_1 \cos(\varphi_1)}{\sqrt{\beta_1}} + \frac{D_2 \sin(\varphi_1 + \Delta\varphi) + \tilde{D}_2 \cos(\varphi_1 + \Delta\varphi)}{\sqrt{\beta_2}} \right) \end{aligned}$$

(A7)

If we introduce

$$x_1 = \sqrt{\epsilon\beta_1}\cos(\varphi_1), \qquad \tilde{x}_1 = -\sqrt{\epsilon\beta_1}\sin(\varphi_1)$$

and define A_1 and B_1 by

$$dL = A_1\, x_1 + B_1\, \tilde{x}_1 \tag{A8}$$

we obtain finally

$$A_1 = \frac{D_2\sin(\Delta\varphi) + \tilde{D}_2\cos(\Delta\varphi)}{\sqrt{\beta_1\beta_2}} - \frac{\tilde{D}_1}{\beta_1} \tag{A9}$$

$$B_1 = \frac{\tilde{D}_2\sin(\Delta\varphi) - D_2\cos(\Delta\varphi)}{\sqrt{\beta_1\beta_2}} + \frac{D_1}{\beta_1} \tag{A10}$$

If we define $\bar{A}_1$ and $\bar{B}_1$ by

$$dL = \bar{A}_1\, x_2 + \bar{B}_1\, \tilde{x}_2 \tag{A11}$$

we obtain

$$\bar{A}_1 = \frac{D_1\sin(\Delta\varphi) - \tilde{D}_1\cos(\Delta\varphi)}{\sqrt{\beta_1\beta_2}} + \frac{\tilde{D}_2}{\beta_2} \tag{A12}$$

$$\bar{B}_1 = \frac{D_1\cos(\Delta\varphi) + \tilde{D}_1\sin(\Delta\varphi)}{\sqrt{\beta_1\beta_2}} - \frac{D_2}{\beta_2} \tag{A13}$$

Fig. 1 Maximum horizontal amplitudes vs horizontal tune with a horizontal crossing angle of $2\phi = 15\,\mathrm{mrad}$ ($\phi\,\sigma_s/\sigma_x = 0.4$)
a) without crab cavities, b) with transverse crab cavities

Fig. 2 Maximum vertical amplitudes vs vertical tune with a vertical crossing angle of $2\phi = 15\,\mathrm{mrad}$ ($\phi\,\sigma_s/\sigma_y = 10.$)
a) without crab cavities, b) with transverse crab cavities

Fig. 3 Maximum vertical amplitudes vs vertical tune with a vertical crossing angle of $2\phi = 0.6\,\mathrm{mrad}$ ($\phi\,\sigma_s/\sigma_y = 0.4$)
a) without crab cavities, b) with transverse crab cavities

Fig. 4 Maximum horizontal amplitudes vs horizontal tune with a horizontal crossing angle of $2\phi = 3\,\mathrm{mrad}$ ($\phi\,\sigma_s/\sigma_x = 0.08$)
a) without crab cavities, b) with transverse crab cavities

Fig. 5 Root mean square deviation vs horizontal tune
a) without crab cavities, b) with transverse crab cavities

Fig. 6 Maximum amplitudes vs horizontal tune on the resonance $\nu_x = (1 + \nu_s)/3$ for different voltages of the transverse crab cavities varying from 0 to the nominal value.

Fig. 7 Maximum amplitudes vs horizontal tune on several resonances for different voltages of the transverse crab cavities varying from 0 to the nominal value.

Fig. 8 Maximum amplitudes vs voltage of the transverse crab cavities for two initial amplitudes ($3\sigma_x, 6\sigma_x$) on the resonance $\nu_x = (1 + \nu_s)/3$

Fig. 9 Maximum amplitudes vs phase distance of the transverse crab cavities from the interaction point for two initial amplitudes ($3\sigma_x, 6\sigma_x$) on the resonance $\nu_x = (1 + \nu_s)/3$

Fig. 10 Maximum amplitudes vs voltage of the transverse crab cavities for two initial amplitudes ($3\sigma_x, 6\sigma_x$) on the resonances shown in Fig. 7

Fig. 11 Maximum amplitudes vs phase distance of the transverse crab cavities from the interaction point for two initial amplitudes ($3\sigma_x, 6\sigma_x$) on the resonances shown in Fig. 7

Fig. 12 Maximum amplitudes vs horizontal tune for different voltages in one transverse crab cavity varying from 90% to its nominal value on the satellite resonance $\nu_x + \nu_s = n$

Fig. 13 Maximum amplitudes vs horizontal tune for different voltages in one transverse crab cavity varying from 90% to its nominal value on the satellite resonance $\nu_x - \nu_s = n$

Fig. 14 Maximum amplitudes vs horizontal tune on several resonances for different voltages of the accelerating cavities varying from 0 to the nominal value.

Fig. 15 Maximum amplitudes vs voltage of the accelerating cavities for two initial amplitudes ($3\sigma_x, 6\sigma_x$) on the resonance shown in Fig. 14

Fig. 16 Maximum amplitudes vs phase distance of the dispersion in the accelerating cavities from the interaction point for two initial amplitudes ($3\sigma_x, 6\sigma_x$) on the resonances shown in Fig. 14

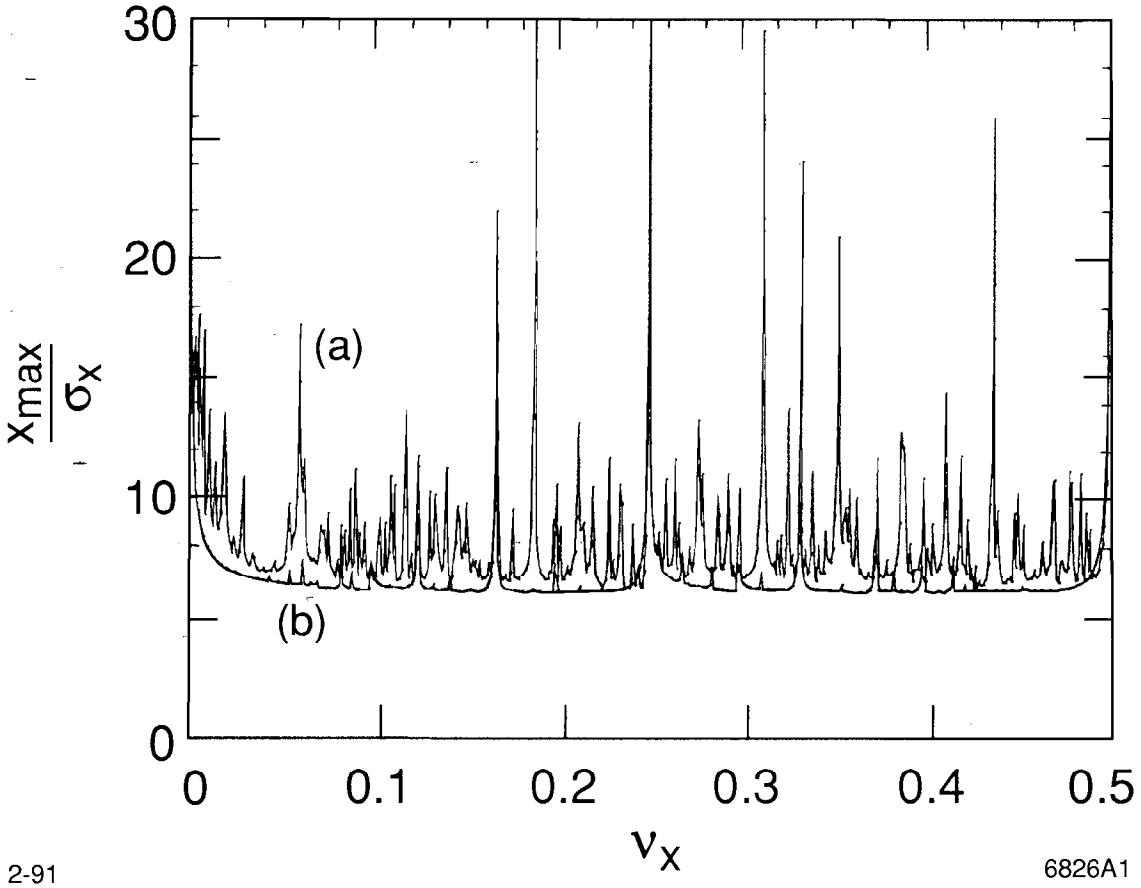

Fig. 1

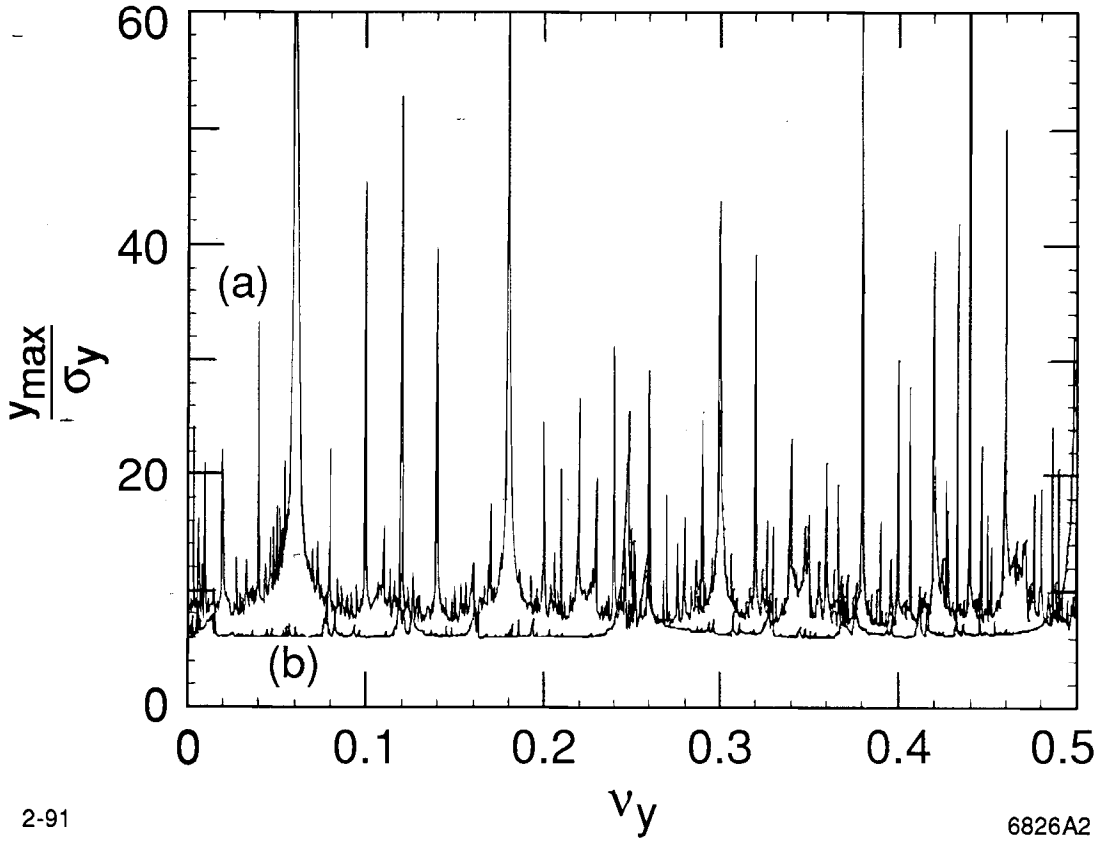

Fig. 2

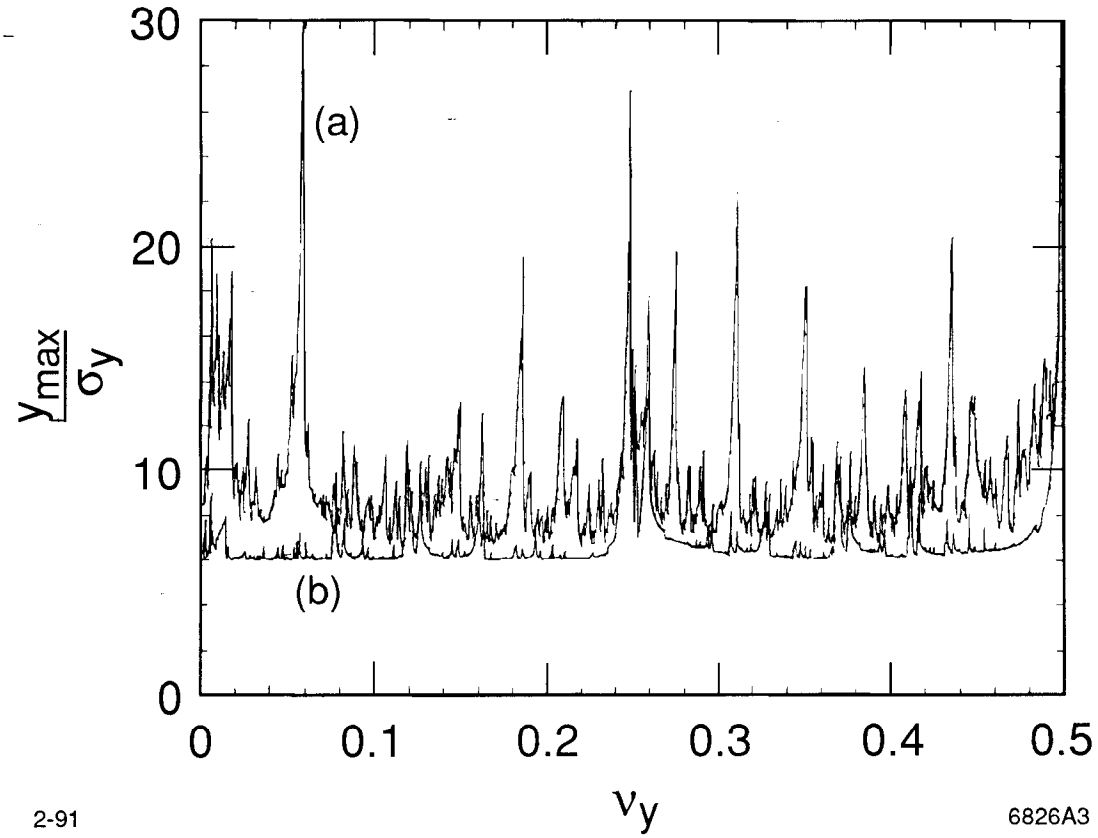

Fig. 3

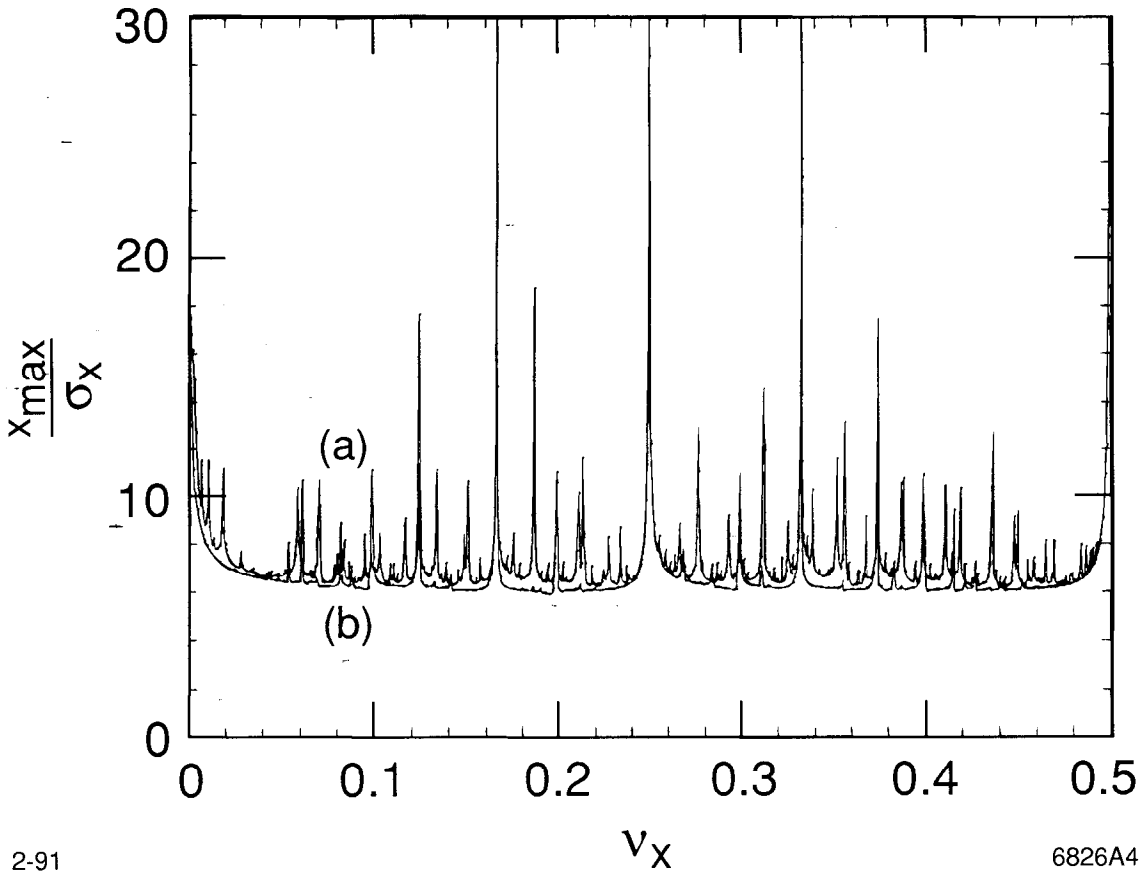

Fig. 4

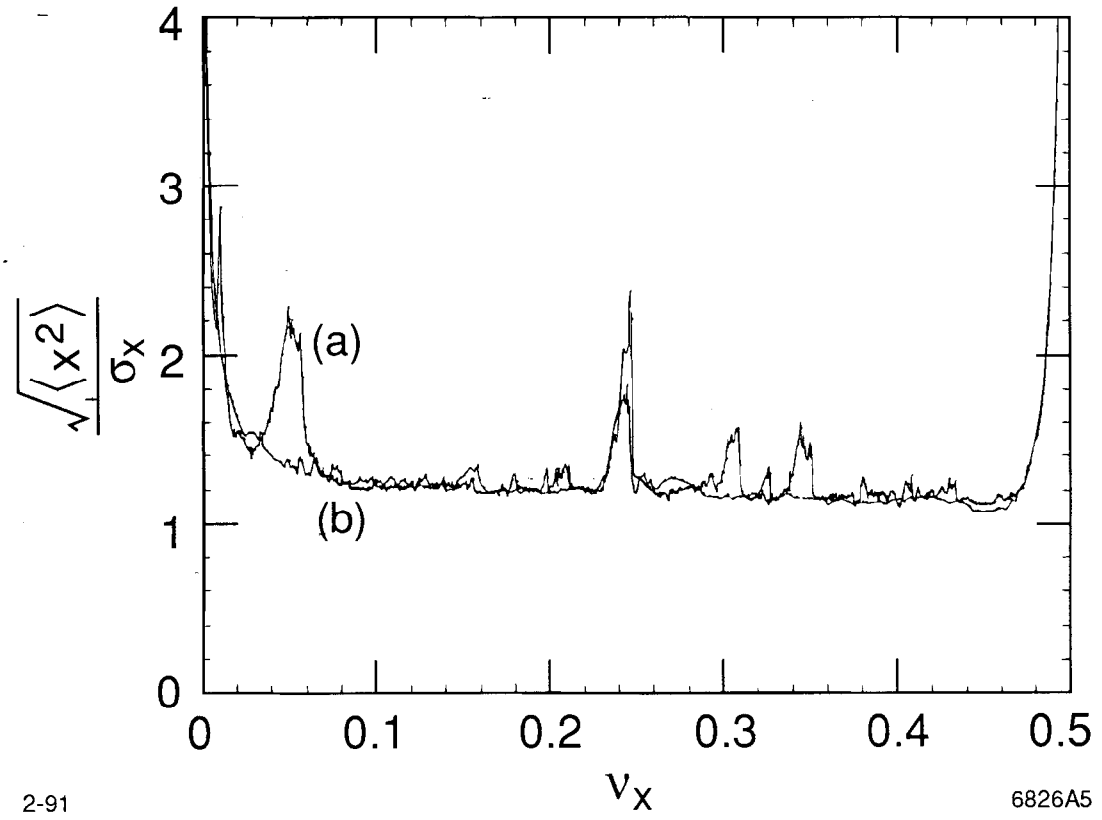
4
3
2
1
0
0
0.1
0.2
0.3
0.4
0.5
$\sqrt{\langle x^2 \rangle}/\sigma_x$
(a)
(b)
ν_x
2-91
6826A5

Fig. 5

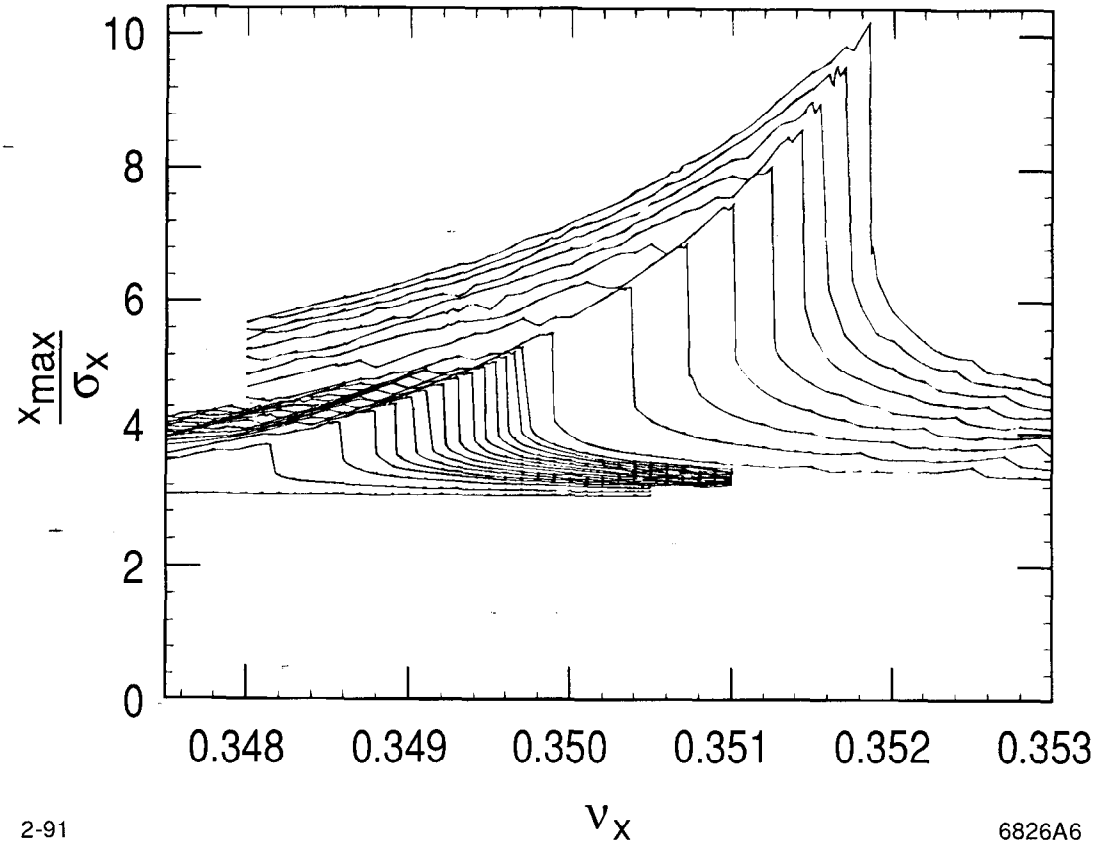
10
8
6
4
2
0
$\frac{x_{max}}{\sigma_x}$
0.348
0.349
0.350
0.351
0.352
0.353
ν_x
2-91
6826A6

Fig. 6

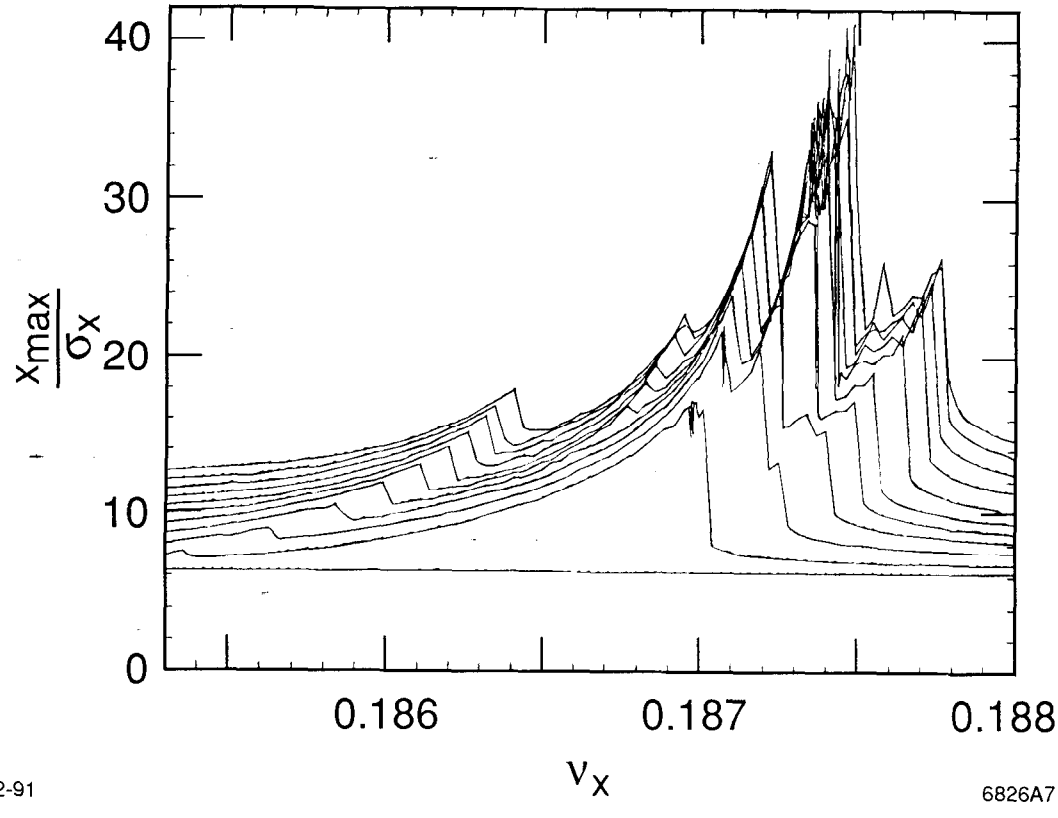

Fig. 7

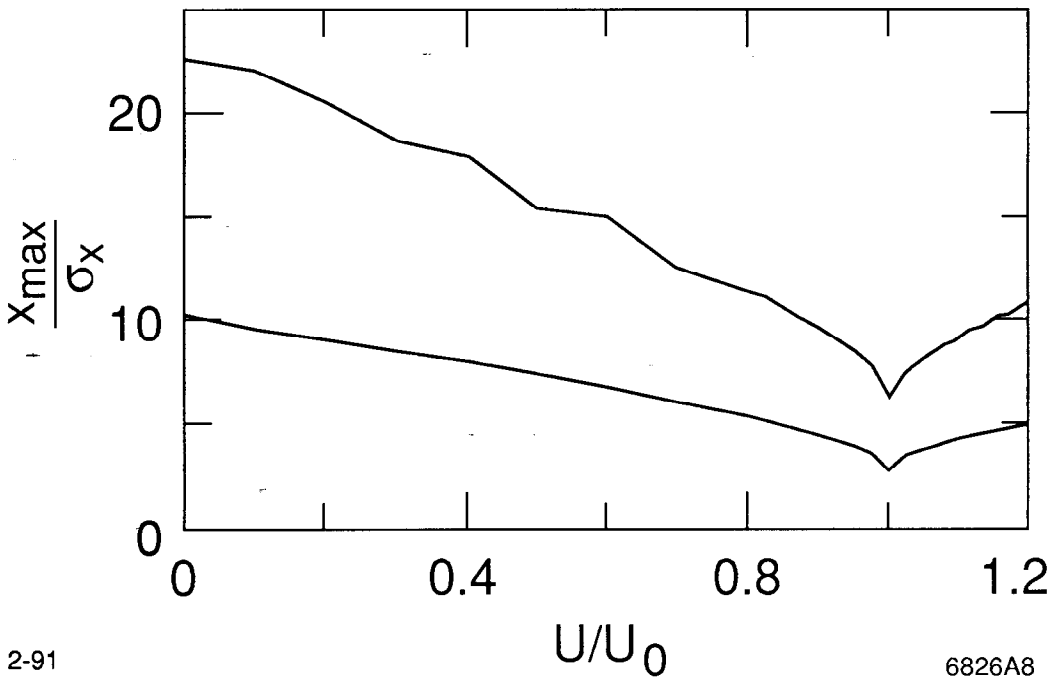

Fig. 8

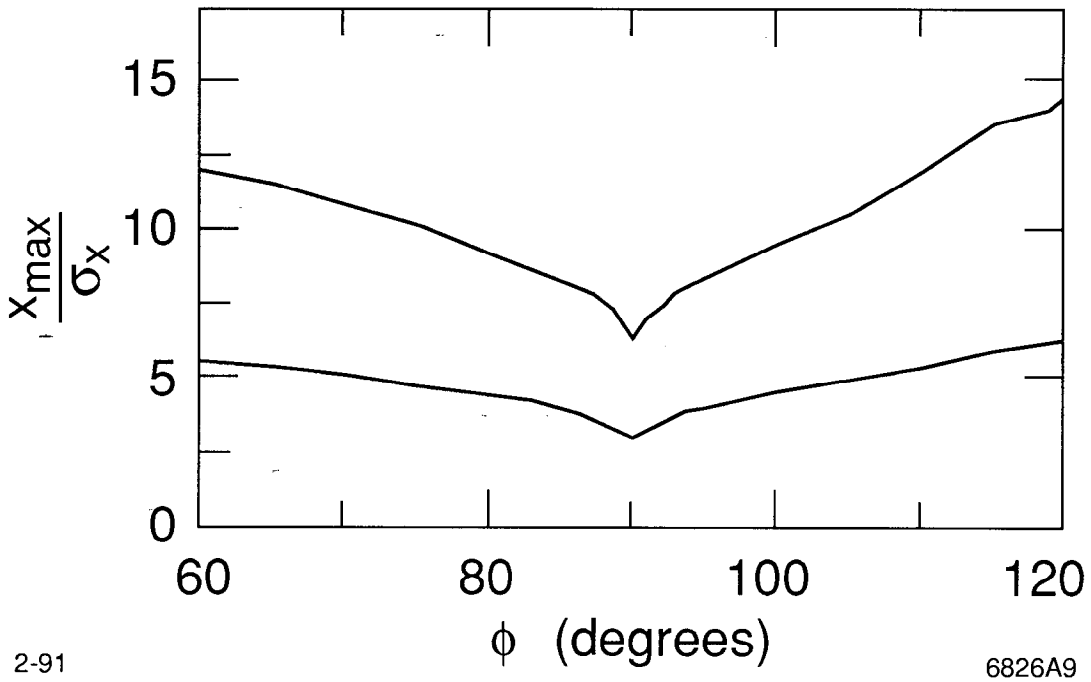

Fig. 9

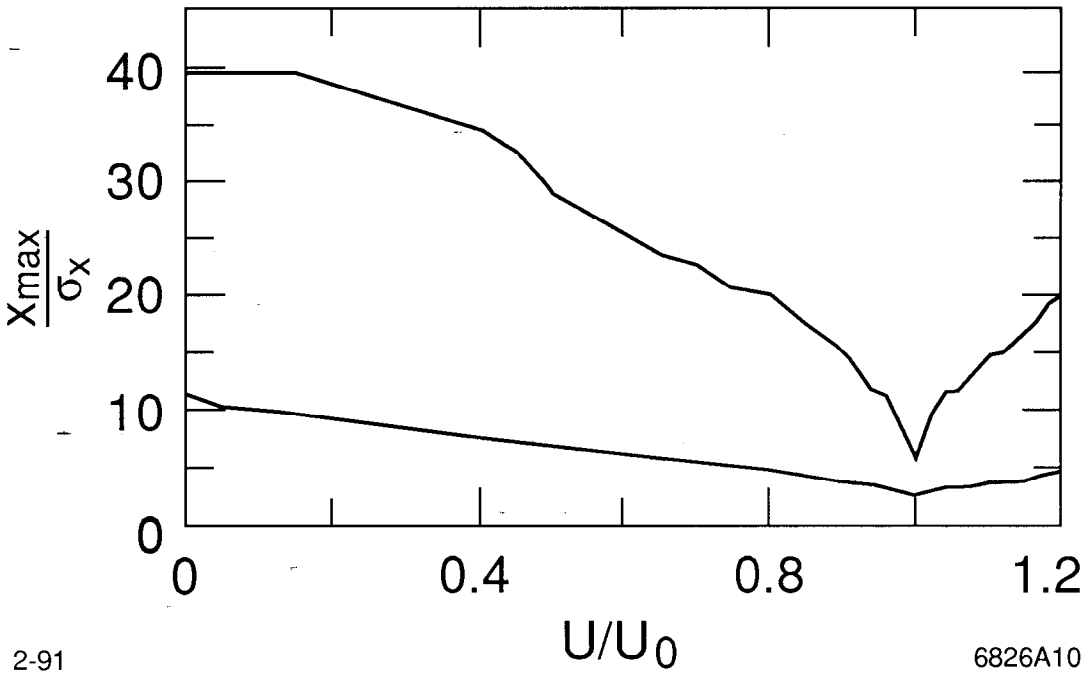

Fig. 10

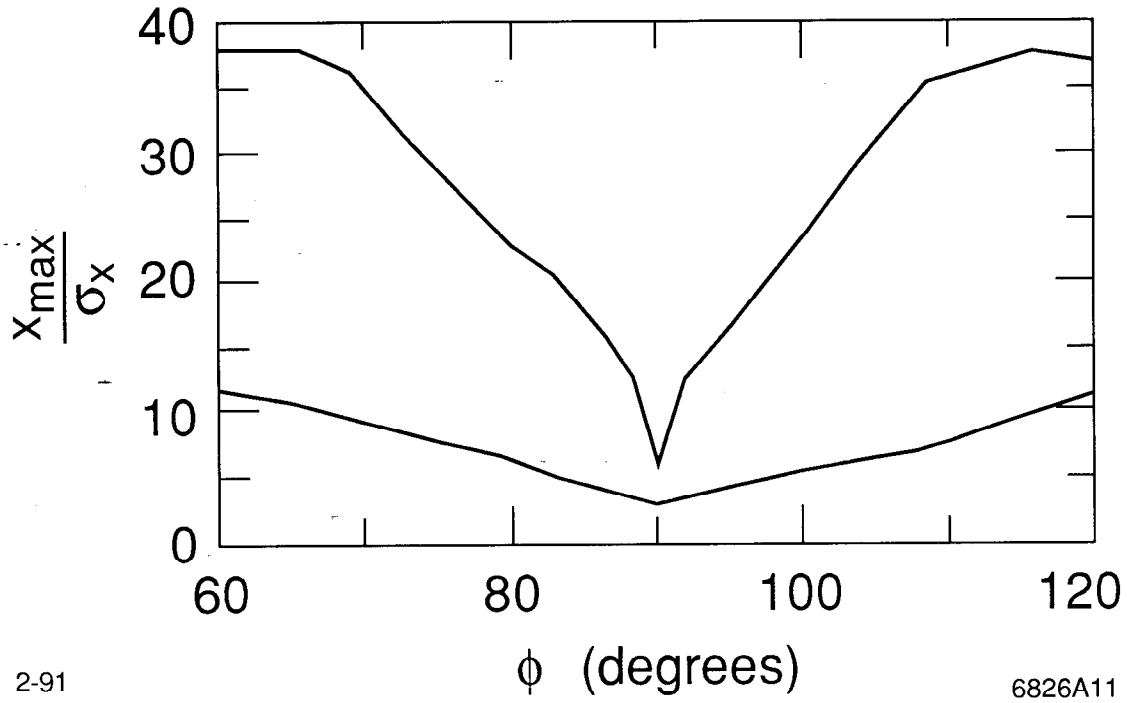
40
30
20
10
0
$\frac{x_{max}}{\sigma_x}$
60
80
100
120
ϕ (degrees)
2-91
6826A11

Fig. 11

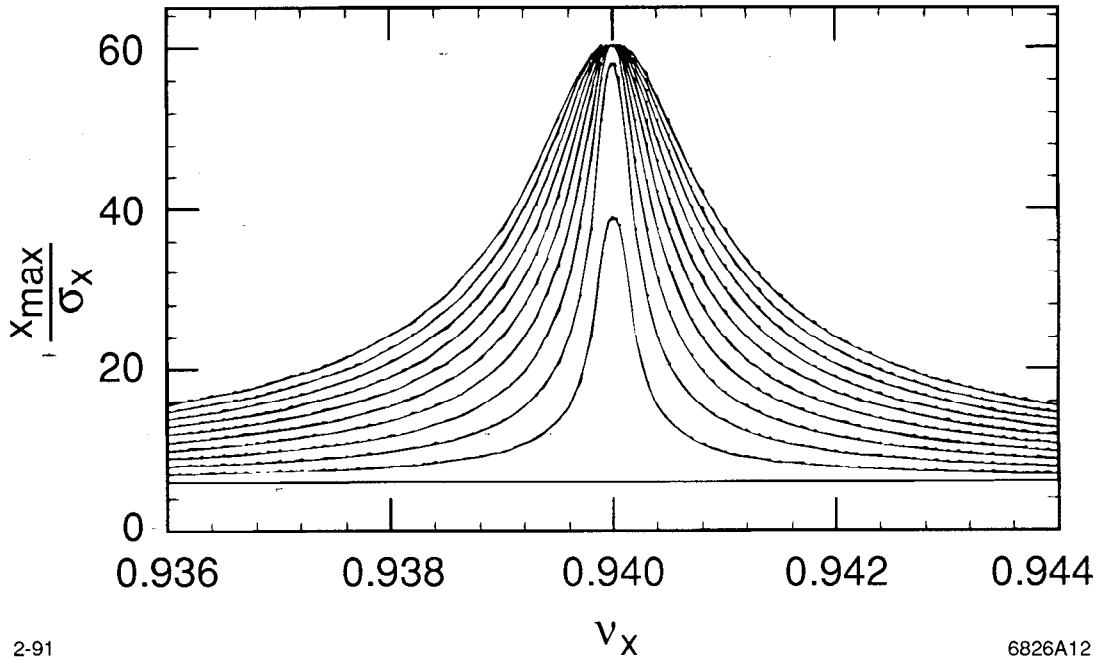
60
40
20
0
$\frac{x_{max}}{\sigma_x}$
0.936
0.938
0.940
0.942
0.944
ν_x
2-91
6826A12

Fig. 12

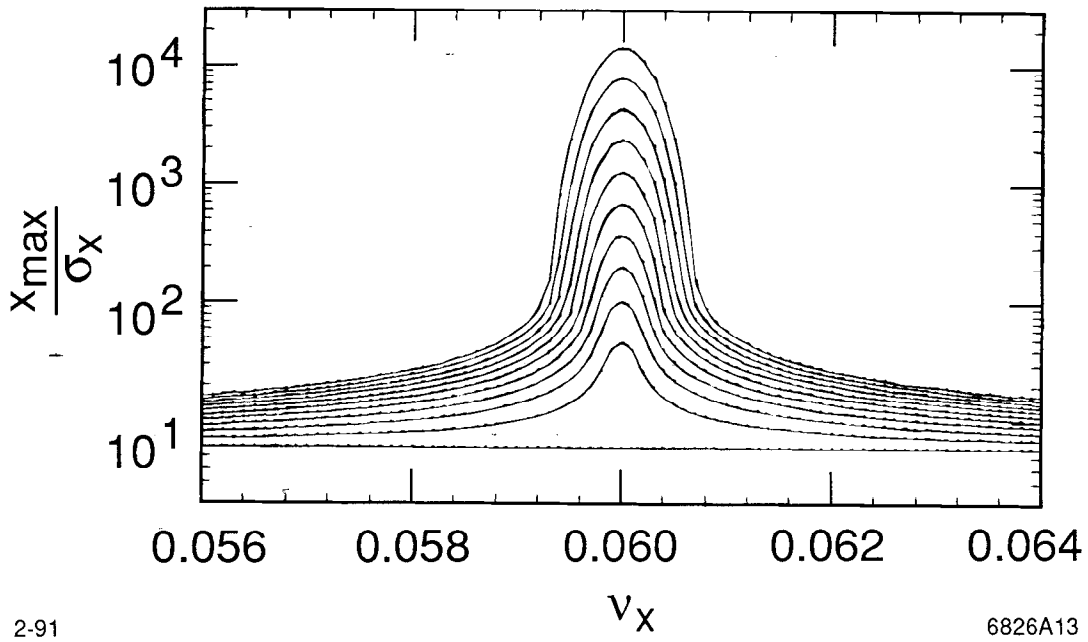
10^4
10^3
10^2
10^1
$\frac{x_{max}}{\sigma_x}$
0.056
0.058
0.060
0.062
0.064
ν_x
2-91
6826A13

Fig. 13

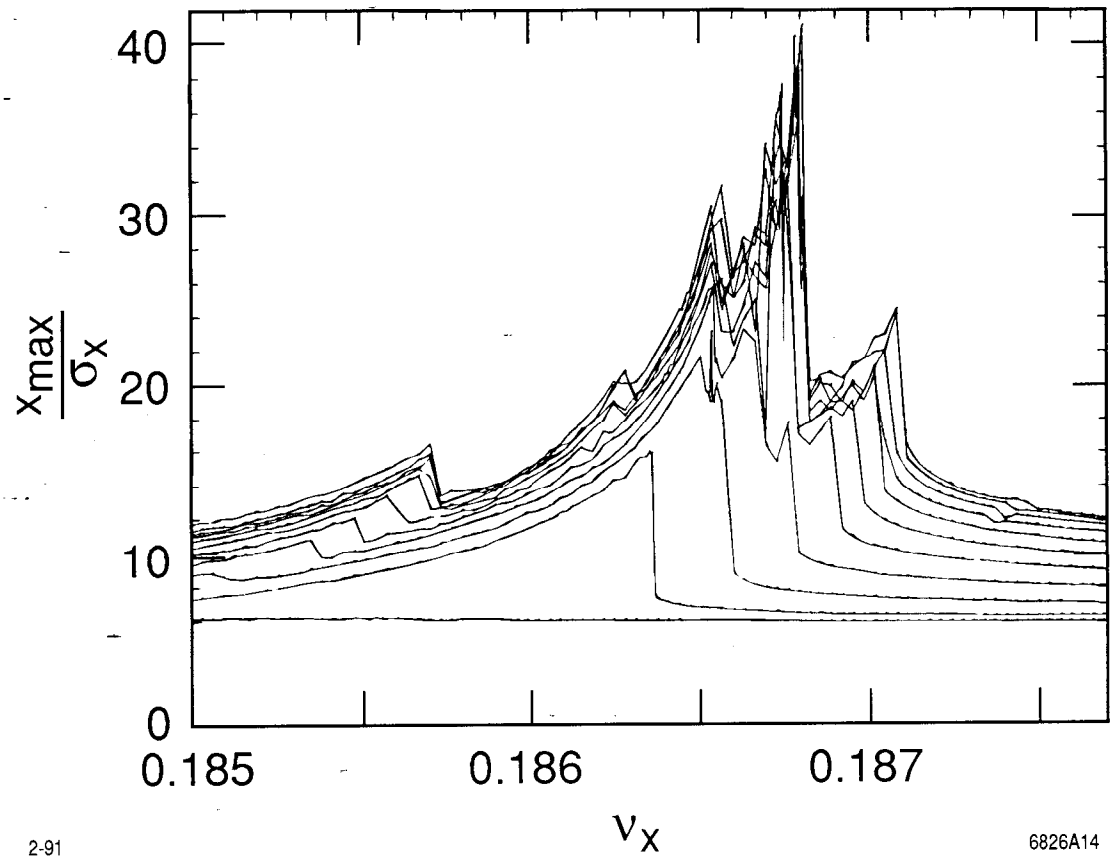

Fig. 14

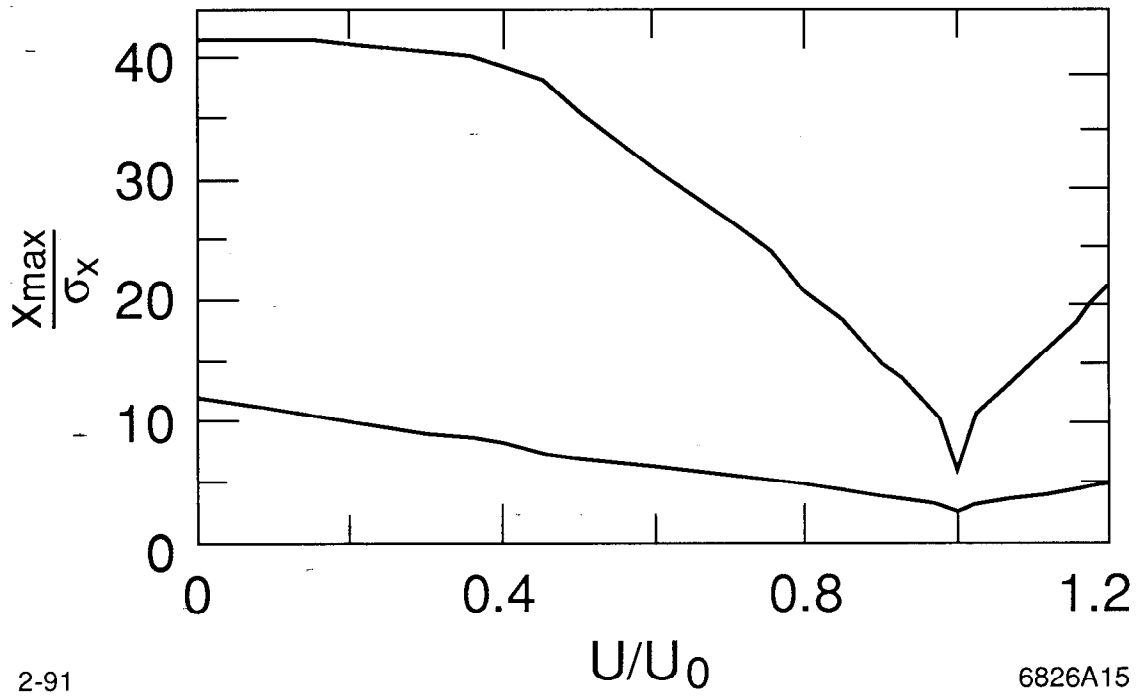

Fig. 15

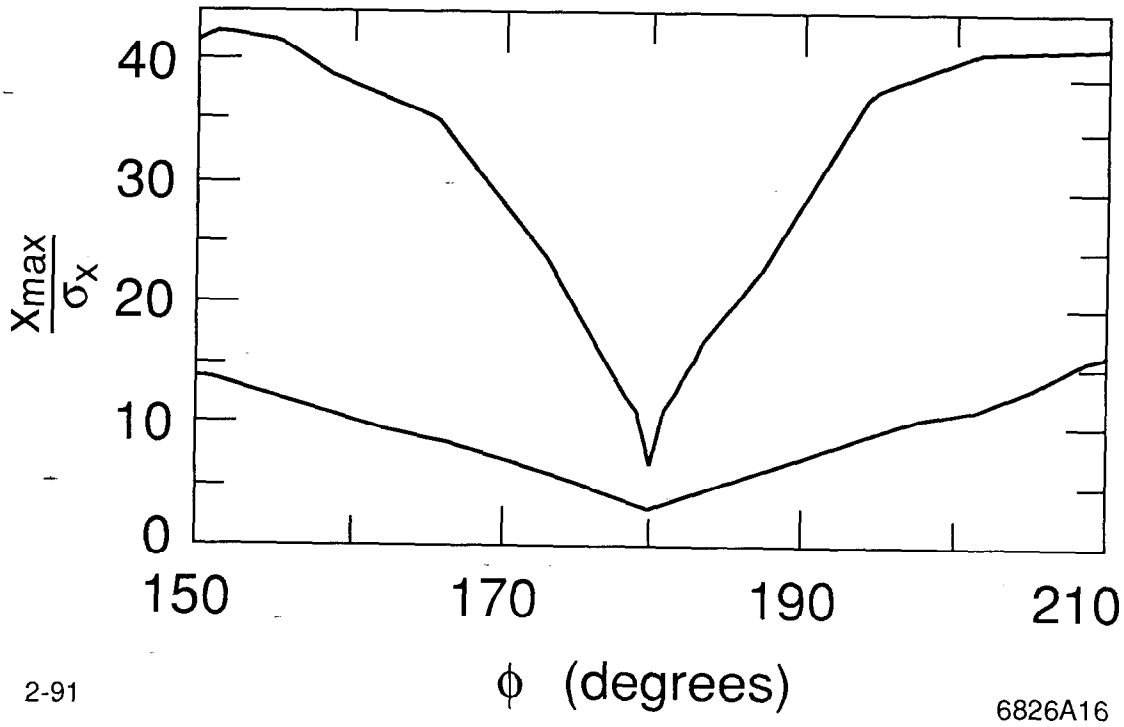
40
30
20
10
0
$\frac{X_{max}}{\sigma_x}$
150
170
190
210
ϕ (degrees)
2-91
6826A16

Fig. 16